This document is the accepted manuscript version of the following article:
Moeck, C., Radny, D., Auckenthaler, A., Berg, M., Hollender, J., & Schirmer, M. (2017).
Estimating the spatial distribution of artificial groundwater recharge using multiple tracers.
Isotopes in Environmental and Health Studies, 53(5), 484-499.

https://doi.org/10.1080/10256016.2017.1334651

Estimating the spatial distribution of artificial groundwater recharge using multiple tracers

Christian Moeck[1], Dirk Radny[1], Adrian Auckenthaler[2], Michael Berg[1], Juliane Hollender[1,4], Mario Schirmer [1,3]

Contact: Christian.moeck@eawag.ch

[1] Eawag, Swiss Federal Institute of Aquatic Science and Technology, Dübendorf, Switzerland

[2] Office of Environmental Protection and Energy, Canton Basel-Country, Switzerland

[3] Centre of Hydrogeology and Geothermics (CHYN), University of Neuchâtel, Neuchâtel, Switzerland

[4] Institute of Biogeochemistry and Pollutant Dynamics, ETH Zürich, Zürich, Switzerland

Keywords: Managed aquifer recharge, Urban hydrogeology, Hydrochemistry, Stable water isotopes, Organic micropollutants, Groundwater mixing

Abstract

Stable water isotopes, organic micropollutants and hydrochemistry data such as main ions are powerful tools to identify different water types in areas where knowledge of the spatial distribution of different groundwater is critical for water resources management. An important question is how the assessments will change if only one or a subset of these tracers is used. In this study, we estimate spatial artificial infiltration along an infiltration system with discharge - river stage relationships and classify different water types based on the mentioned hydrochemistry data for a drinking water production area. Managed aquifer recharge with surface water into the aquifer is used to create a hydraulic barrier between contaminated groundwater and drinking water wells. We systematically compare the information content from the applied tracers and illustrate the differences in distribution and calculated mixing ratios. Despite uncertainties in the mixing ratio the overall spatial distribution of artificial infiltration is very similar for all tracers. Highest infiltration occurred in the eastern part of the infiltration system whereas at the western part infiltration is low. A more balanced infiltration within the infiltration system could lead to a better distribution of the elevated groundwater mound, preventing natural inflow of potentially contaminated groundwater.

1. Introduction

Water supply in urban areas with long industrial history is challenging due to high water demand of population and industry [1]. Furthermore, groundwater contamination and areas potentially affecting the water quality makes water supply a very complex issue [2, 3, 4]. To realize the water demand and protect water resources, groundwater recharge plays an important role [5]. However, where natural recharge rates are too small, managed aquifer recharge (MAR) can be a measure to provide a water surplus and to dilute potentially contaminated groundwater [6]. Moreover, MAR can lead to an elevated groundwater mound, which serves as a barrier preventing natural inflow of potentially contaminated water coming from adjacent areas [7, 8]. Therefore, knowledge of flow paths and distribution of artificial infiltration is essential for adequate groundwater management [9, 10]. A solid understanding of flow processes in the subsurface and associated uncertainties are further required for mathematical model predictions to simulate for instance changing boundary conditions and to optimise the water supply system. Although a comprehensive description of all subsurface heterogeneities is never obtainable [11, 12, 13], a solid process understanding is crucial for water management strategies.

Typically, tracers are used to gain information about subsurface processes. For instance, stable water isotopes, organic micropollutants and hydrochemistry data such as main cations and anions are known to be powerful tools to identify the distribution of different water types in areas where detailed knowledge of artificial infiltration distribution is critical for water resources [14, 15, 16]. Variations in stable water isotopes (e.g. oxygen-18 ($\delta\ ^{18}O$) and deuterium ($\delta\ ^{2}H$)) within the groundwater samples can be used to create an interrelationship between groundwater and the source of origin [15, 17]. Since the composition of stable water isotopes is typically not altered in the aquifer by water-rock interactions it is another tool to understand mechanisms of groundwater circulation such as mixing between different water types. Present pollutions in surface water or groundwater can be additionally used to understand subsurface processes [18, 19]. Although these contaminations are typically unwanted in the aquifer, they can provide insights into flow and transport processes [20]. Anthropogenic markers such as artificial sweeteners (e.g. acesulfame) are increasingly used, especially in the context of infiltration with surface water into the groundwater [21, 22, 23, 24, 25]. The use of these indicator substances allows determining specific pathways [26, 27] because higher concentrations can be found usually in effluent dominated river water, and thus can be used as a tracer to estimate the interaction between surface water and groundwater [28, 29].

According to Massmann et al. [30] and Gasser et al. [31] the application of multiple tracers offer more insight than from a single tracer and is required to quantify uncertainty due to aquifer heterogeneity and different subsurface processes. The interpretation of subsurface processes based on multiple tracers is however less common [32]. Therefore, we systematically investigate the effects of using different tracers to identify the spatial distribution of artificially infiltrated water for a study area in northern Switzerland. Here drinking water production is in an urban area with different landfills and industrial zones. Groundwater is artificially recharged by infiltrating water from the river Rhine by an excavated system of channels and ponds and lead to an elevated groundwater mound, which serves as a barrier to prevent inflow of contaminated regional groundwater. However, a range of chlorinated solvents were measured in the abstracted groundwater. Therefore, it is essential to have detail knowledge about the temporal and spatial infiltration pattern at the study site. It is expected that in areas where infiltration rates are low, the regional groundwater component is dominating the water composition. Using solely total infiltration rates as an indicator for the elevated groundwater mound will not provide the required information about the spatial pattern. Moreover, using groundwater levels only will not help to identify mixing ratios and possible upwelling through, for instance, factures which seems to be possible due to the geological setup at the study site. Therefore, artificial infiltration rates along a constructed infiltration system were estimated and all aforementioned tracers were acquired during one field sampling campaign. These data were already incorporated in a larger dataset where flow and transport processes were identified by a multivariate statistical analysis [32]. In this study aquifer mixing in the subsurface is identified, where a higher amount of artificial infiltrated surface water is mixed with water originating from the regional flow pathway in the vicinity of the drinking water wells. Although the groundwater mixing was identified the spatial distribution and mixing ratios were uncertain and were not investigated systematically. Furthermore, the highest potential risk for drinking water supply was estimated in the western part of the study area where fractures exist. The authors state that particular wells with a higher proportion of regional water coming most likely from the south should be further investigated. Following this suggestion, we calculate mixing ratios based on selected water type endmembers and subsequently spatial differences in mixing ratio distributions between the different tracers are identified.

2. Study area

The study area is located in north-western Switzerland and is an essential drinking and industrial water site for the region. Two main aquifers namely the Quaternary Rhine gravel and the underlying karstified Upper Muschelkalk limestone aquifer are present, where the Quaternary aquifer is largely used for drinking water production.

The 50-60 m thick limestone of the Muschelkalk represents a highly fractured and karstified aquifer with an average hydraulic conductivity of $1.3*10^{-4}$ m/s [33], ranging between $1*10^{-3}$ m/s and $2*10^{-6}$ m/s [34] depending on the position. The fluvial-glacial gravels from Quaternary strata appear with a varying thickness of 5 to 50 m on top of the bedrocks. The thickness close to the main drinking water wells (i.e. the pumping well gallery, Figure 1) is around 20 to 40 m. The average hydraulic conductivity is $3.1*10^{-3}$ m/s [33].

The regional flow direction is from south to north to the river Rhine. However, the artificial river water infiltration highly influences the groundwater flow (Figure 1). Increasing water demand led to an installation of an artificial groundwater recharge system in 1958 and was further designed in order to maintain a hydraulic gradient towards areas of potential risk (e.g. urban areas, landfills, industrial areas, highways, rail tracks and a harbour for the chemical industry, Figure 1). Surface water is extracted from the river Rhine in the direct vicinity of the study area and a first purification follows directly. Then, the surface water is inducted at the eastern location of the system (Figure 1 and 3) and is distributed in the 3500 m long infiltration channels (area: 7000 m²) and in the six ponds (area: 4000 m²). The distribution of the surface water follows the flow gradient (east to west) and is solely manually adjusted by open or closing different weirs, which also controls the distribution between parallel channels. No return flow can occur due to the topographical downward slope. The ponds are connected through the infiltration channels. Only flow into the ponds can occur due to the topographical slope. No outflow exists for the infiltration system (channels and ponds), which means that all inducted surface water will be artificial infiltrated. The ground of the infiltration channels and ponds contains an approximately 40 cm thick artificial gravel layer to facilitate the infiltration into the subsurface. The inducted amount of surface water into the infiltration system depends on expected water demand, associated with changing extraction rates at the drinking water wells. Currently, the infiltrated volume is 100,000 m^3/d on average which is twice as much water as abstracted [8]. Moreover, large quantities of groundwater are abstracted for industrial purpose east of the study site, and smaller amounts south of the artificial infiltration system. The approximately distance between the infiltration system and drinking water wells in the

north is 400 m. A more detailed description of the geology and hydrogeology can be found in Spottke et al. [33] and Moeck et al. [32].

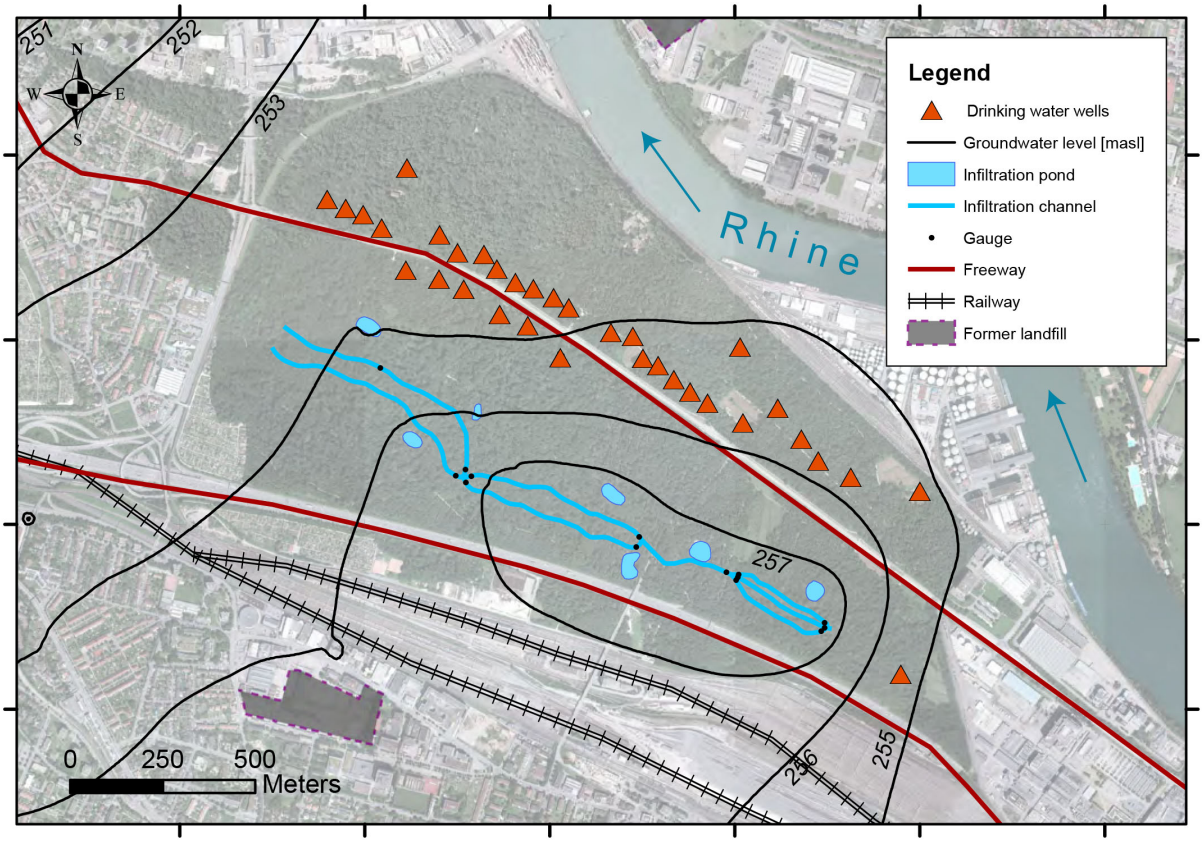

Figure 1: Study area in a highly urbanized region of the River Rhine valley, northern Switzerland. Elevations range from south to north from around 290 meters above sea level (masl) to 250 masl in the vicinity of the Rhine. The northern boundary of the Hardwald is the river Rhine, urban areas and river Birs in the west, railways and industrial areas in the south as well as industrial areas in the East. A highway passes directly through the Hardwald from west to east. Artificial infiltration channels and ponds are shown in -blue. The piezometric heads are shown as black lines.

3. Methods

The water discharge at 14 selected locations in the channels was measured repeatedly over a time span of three months with a magnetic induction water flow meter (Company: Ott, Flow meter type: MF pro) during different discharge conditions. Water levels in the channels were recorded continuously at the selected locations (see figure 1 and 3) that were chosen based on inlet and outlet of the channels. Based on these data a discharge stage relationship was established. In addition, the discharges into the ponds were measured continuously at the inlet

147 of the ponds with a weir system (6 artificial ponds). These data provides directly the inflow
148 rate into the ponds without additional measurements. Note that no outflow in the ponds or
149 channels exists. Subsequently, a water mass balance was calculated for each section between
150 two measurement points where the inflow rate was subtracted by the outflow rate. No
151 infiltration occurred where outflow equalled inflow, whereas infiltration from the channel into
152 the aquifer took place for values larger than zero. For channels with connection to ponds the
153 inflow rate (based on the stage discharge relationship) was first subtracted by the measured
154 inflow at the ponds (based on the weir measurement). The remaining difference was then
155 subtracted by the outflow rate (based on the stage discharge relationship) in a second step.

156 A sampling campaign was conducted in March 2015 with 50 groundwater sampling locations
157 and one Rhine surface water location to quantify the distribution of artificial infiltration. The
158 samples were collected by using stainless steel submersible pumps (Grundfos, MP1), directly
159 from the sampling faucet of the drinking water wells and as grab samples in the infiltration
160 system. The physico-chemical parameters temperature, pH, electrical conductivity, the
161 oxidation-reduction-potential (ORP) and dissolved oxygen concentrations were measured in
162 the field using portable devices (HACH-LANGE, HQ40d). Sample collection was performed
163 after stabilization of the physico-chemical parameters from the wells and piezometers. The
164 water samples were analysed using standardised methods for major cations and anions
165 (Metrohm 761 Compact IC) as well as for the stable water isotope signatures (deuterium
166 (δ^2H) and oxygen ($\delta^{18}O$)) (Picarro L1102-I) and organic micropollutants (online solid phase
167 extraction followed by liquid chromatography coupled with electrospray ionization to high
168 resolution tandem mass spectrometry [35]. The measurement errors for all tracers are
169 provided in table S1.

170 The obtained data were subsequently used to identify water type endmembers and to calculate
171 the mixing ratios of stable isotope composition, cat- and anions and organic micropollutants
172 based on selected endmembers to develop a consistent system understanding. The surface
173 water infiltration represents one endmember. Due to the large amount of artificial infiltration
174 (100,000 m^3/d on average), this endmember strongly controls groundwater flow and
175 composition. The second endmember represents the regional groundwater. Here, the sample
176 with the most distinct differences in all tracers compared to the surface water was selected.
177 Compared to the infiltrated surface water, this selection is uncertain but represents the best
178 guess based on the available data set.

For the stable water isotope, persistent organic micropollutants and cat- and anions the linear mixing was calculated as follows:

$$GW_{Mix} = a \times GW_{Infiltration} + b \times GW_{Regional} \quad (1)$$

$$a + b = 1 \quad (2)$$

$$b = \frac{GW_{Infiltration} - GW_{Mix}}{GW_{Infiltration} - GW_{Regional}} \quad (3)$$

where GW_{Mix} is the isotope (organic micropollutants, or cat- and anion) composition based on the infiltrated Rhine water composition ($GW_{Infiltration}$) and the regional groundwater composition ($GW_{Regional}$). The factors a and b show the portion of infiltrated water (a) and regional water (b) for the sampling location (GW_{Mix}) where mixing occurred. For the cat- and anions the mixing ratio was calculated based on each of the considered cat- and anion. For the latter the cat- and anions were scaled in order to avoid that a single cat- or anion dominates the mixing ratio due to higher concentration differences. Although we are fully aware that precipitation, dissolution and degassing might change the results for the cat- and anions, we chose a simple linear mixing equation due to the relatively short residence times of less than 20 days on average between infiltration channels and pumping wells [36]. The average of 20 days represents the maximum breakthrough, but first arrivals can be observed after one day already. It is assumed that mineral precipitation and dissolution effects are minor. However, at the boundaries of the study area where longer mean residence times are expected, the mineral precipitation and dissolution might affect the mixing ratios. This issue is discussed in the result sections 4.5 and 5. Uncertainty in our results was expressed as the standard deviation of mixing ratios calculated by using all tracers. The same weight for all tracers was used in this calculation to avoid preferences.

4. Results

4.1 Artificial infiltration rates

The following section describes the channel stage-discharge relationships for one measurement location, shown as an example for all other locations. In Figure 2a a linear relationship was established with a high correlation (R) of 0.94. Based on the weekly measurements from 08.2008 to 10.2013, the variations in channel stages were relatively small (Figure 2b), corresponding to a discharge rate of 0.3±0.05 m^3/s at the entrance point of the infiltration channel (range 0.23 m^3/s and 0.37 m^3/s, Figure 2c).

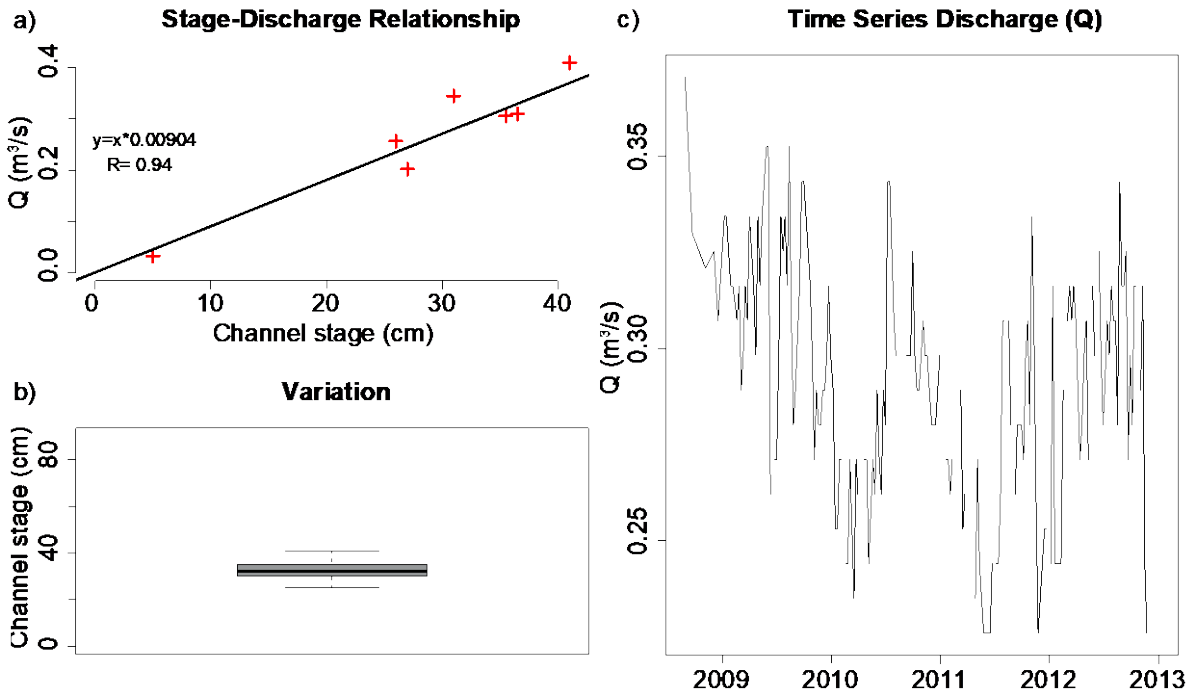

Figure 2: a) Linear channel stage-discharge relationship based on seven measurements (red crosses), b) Boxplot of the weekly channel stage variation without the seven measurements of figure 2a, c) Calculated time series of discharge at the measurement location based on obtained equations from the stage-discharge relationships.

Based on the obtained discharge time series for each of the 21 locations a mass balance was calculated for each section between two measurement points. Figure 3 shows the time series for the 13 sections as well as the total infiltrated amount of Rhine river water. In cases were the sum was zero (blue colour) no infiltration occurred between the measurement points whereas values larger than zero indicate infiltration loss. The highest infiltration (red colour) occurred at section 5, where the infiltration pond 6 is located (Fig. 3). Followed by infiltration at section 7, where the infiltration pond 5 can be found. These two ponds located in the Eastern part of the infiltration system, dominates strongly the infiltration regime. In the western part of the infiltration system the infiltration rate is visibly smaller (Sections 8-13). Clearly, most artificial recharge occurred in the Eastern part of the infiltration system. Although smaller temporal variability for some sections can be observed, the infiltration rates are relatively stable in time and location.

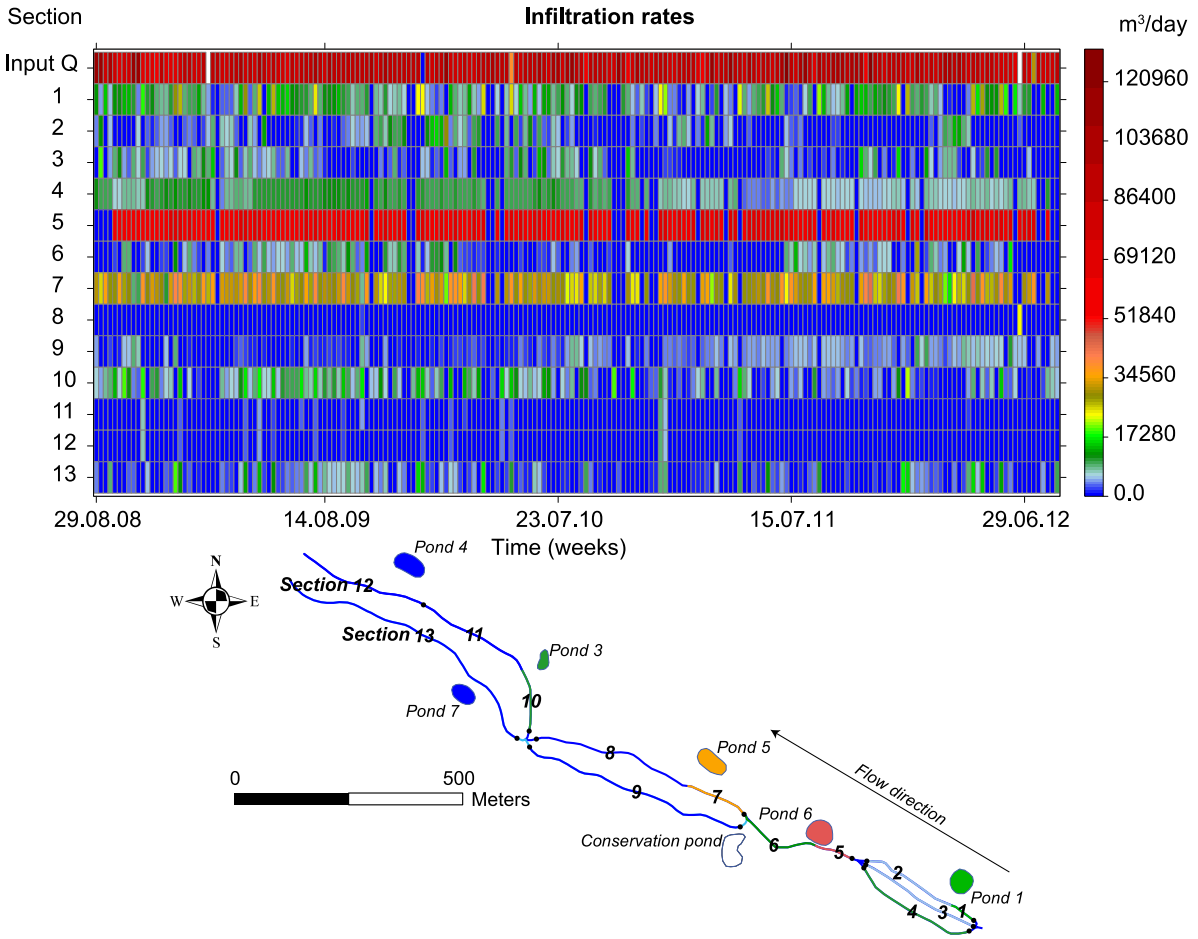

Figure 3: Top panel: Time series of total supply in the infiltration system (Input Q) and artificial groundwater recharge for each section. Blue colours shows no or small recharge rates whereas red colours indicate greater infiltration loss. Bottom panel: Artificial infiltration system with each section and infiltration channels (lines) and ponds (polygon).The colours for each section shows the average recharge rate, where blue colours shows no or small recharge rates whereas red colours indicate greater infiltration loss. The supply is in the south east and flow direction is to north west.

4.2 Stable water isotopes

Stable water isotope signatures, namely $\delta^{18}O$ and $\delta^{2}H$ were used to determine the endmembers $GW_{Infiltration}$ and $GW_{Regional}$ applied for the calculation of mixing ratios. Because stable water isotopes are not altered in the groundwater by aquifer matrix-water interactions, they are a suitable tool to evaluate groundwater mixing [17, 37]. The stable water isotope composition was between -11.3 to -8.7‰ ($\delta^{18}O$) and -81.5 to -64.0‰ ($\delta^{2}H$). All samples follow the local meteoric water line (LMWL). Most samples show a similar stable water isotope composition compared to the infiltrated Rhine river water. Samples indicating regional groundwater have however, an enriched isotope composition, indicating different

water origins and associated mean groundwater ages. After Moeck et al. [32] the isotope composition of $GW_{Regional}$ is indicative of Muschelkalk water, which is in line with the geological model for the study area. Sampling locations between the two endmembers represent mixtures of different fractions. The mixing ratios will be discussed in section 4.5.

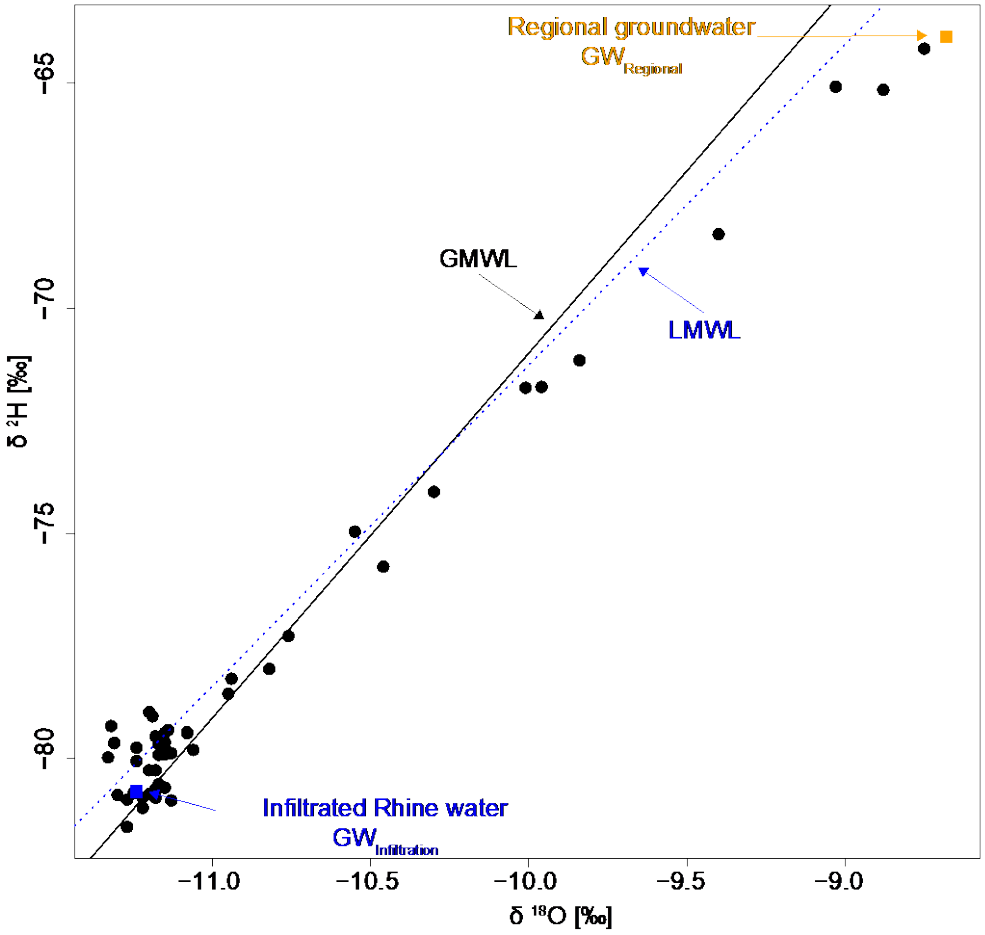

Figure 4: $\delta^{18}O$ - $\delta^{2}H$ [‰] diagram with the acquired data during the sampling campaign. The black line shows the Global Meteoric Water Line (GMWL) and the dotted blue the Local Meteoric Water Line (LMWL).The GMWL was based on the work of [38], whereas the LMWL was based on time series of precipitation from Basel. The black dots represent individual samples. The Rhine surface water composition ($GW_{infiltration}$) is displayed with blue colour and the selected regional water composition ($GW_{regional}$) is shown in orange colour. Both samples show the isotope composition obtained during the sampling campaign. It is assumed that the fluctuation in the isotope compositions in the bedrock is minor. The range of Rhine water isotopes is between -11.4 to -10.3 ‰ for $\delta^{18}O$ and -81.8 to -74.1 ‰ for $\delta^{2}H$.

260 **4.3 Organic micropollutants**

261 Anthropogenic markers are increasingly used in the context of (artificial) infiltration with
262 surface water into the groundwater due to the commonly persistent behaviour. In the
263 following, we present the relationship between the stable water isotope signatures $\delta^{18}O$ with
264 carbamazepine. Carbamazepine, an antiepileptic and antidepressant drug is very persistent to
265 biodegradation [29, 31] and shows a good correlation with other persistent tracers such as the
266 artificial sweetener acesulfame [39].

267 As shown in Figure 5, higher concentrations of carbamazepine are present in the infiltrated
268 Rhine river water that also has lower values in stable isotope signatures. Sampling locations
269 with higher concentrations of carbamazepine show a strong influence of the artificially
270 infiltrated water. In contrast, the selected endmembers for the regional groundwater
271 composition show a low concentration of carbamazepine (under the detection limit of 2 ng/L)
272 associated with an enriched isotope composition, indicating that no mixing with surface water
273 occurs. The different water origin of the regional groundwater, likely Muschelkalk water, is
274 validated by the absence of organic micropollutants. The sampling locations between the two
275 endmembers represent mixtures with different fractions, indicating a lesser amount of
276 artificial infiltrated Rhine water. Note that two samples have higher concentrations than the
277 $GW_{Infiltration}$ endmember which is probably related to the sampling strategy. The infiltrated
278 Rhine river water was collected as a 24 hour mixing sample whereas each sampling point in
279 the field was acquired as a single sample. It is known that the Rhine river water has some
280 variability in the concentration load during the day and this might explain the small
281 differences between $GW_{Infiltration}$ and the two samples with higher concentration. During
282 our sampling champagne precipitation occurred in the study area and could have led to higher
283 variability in the water composition during the day compared to dry weather conditions.
284 Furthermore, the 24 hour mixing sample of river Rhine water does not correspond completely
285 the water composition at the pumping wells due to transport processes in the aquifer which
286 are around 20 days until the maximum breakthrough occurred.

287

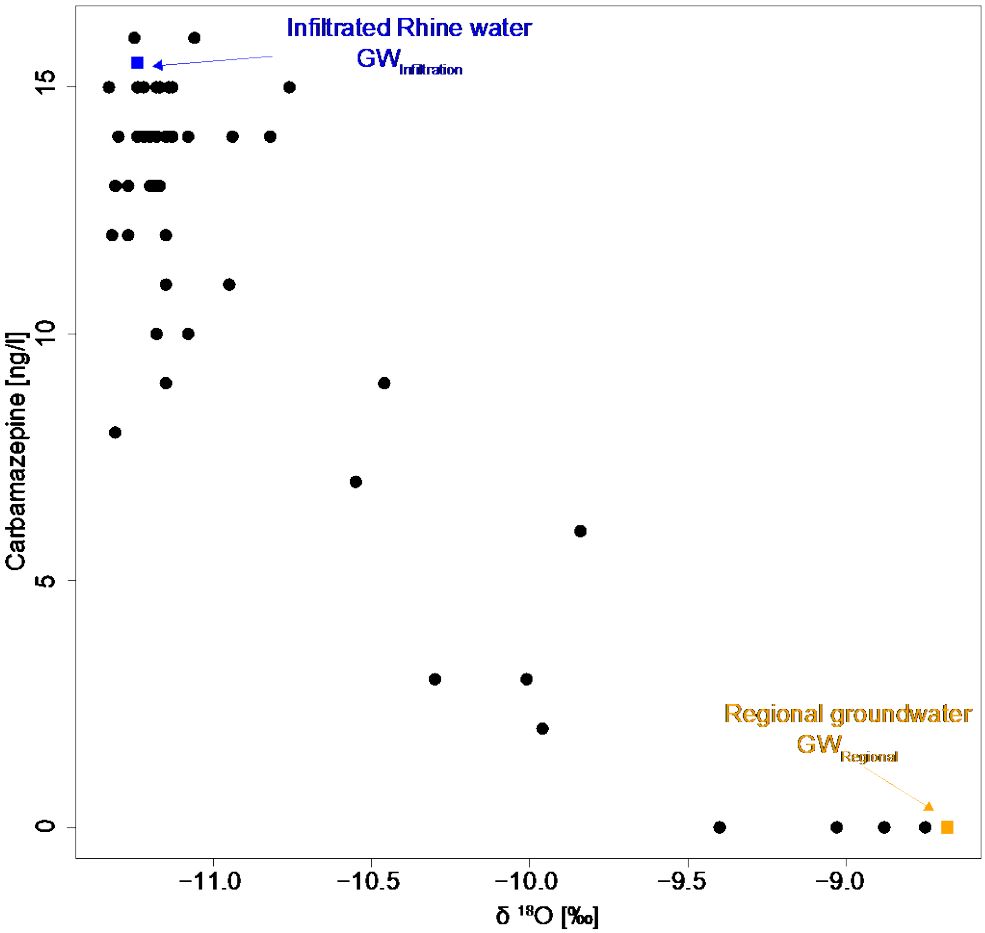

Figure 5: $\delta^{18}O$[‰] – Carbamazepine [ng/l] diagram where the black dots represent individual samples. The Rhine surface water composition ($GW_{infiltration}$) is displayed with blue colour and the selected regional water composition ($GW_{regional}$) is shown in orange colour

4.4 Hydrochemistry data

Bivariate plots of Ca^{2+} and Na^{+} as well as of HCO_3^{-} and SO_4^{2} are shown in Figure 6. These cations and anions were chosen because they show the highest variability in terms of standard deviation between all samples [32]. The infiltrated Rhine water has relatively low concentrations in cations and anions compared to the groundwater samples, with regional groundwater (second endmember) showing considerably higher mineralization. Especially, higher concentrations can be found for Ca^{2+} and HCO_3^{-} likely indicating Ca-rich mineral dissolution due to the existing Muschelkalk limestone. One sample (21.C.206) shows a different concentration, located at the western edge of the study area where concentrations for all hydrochemistry parameter are highest (Table S2, supplemental online material). This sampling point is directly situated at the Rhine Valley Flexure zone and might indicated vertical exchange and upwelling of waters originating from the salt and gypsum layer [32].

Therefore, this sampling point must be interpreted with caution and is not included for the calculation of the mixing ratios based on cations and anions.

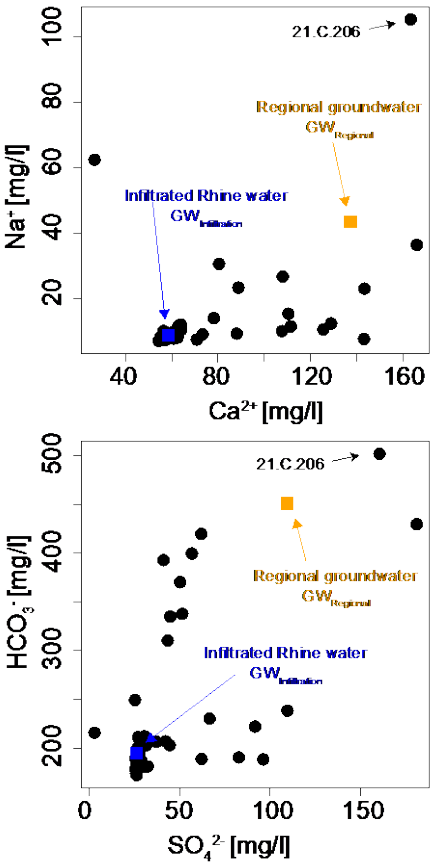

Figure 6: Relationship between cations Ca^{2+} and Na^{+} and anions SO_4^{2-} and HCO_3^{-}. The black dots represent individual samples whereas the regional water composition ($GW_{regional}$) and the Rhine water composition ($GW_{infiltration}$) are printed in yellow and blue colours, respectively.

4.5 Calculated mixing ratios

The calculated mixing ratios are provided in Table S3 (supplemental online material) and indicate similarities in the mixing ratio for most of the sampling points by using the different tracers. For instance, the sampling location 21.J.102, a multilevel piezometer, shows a high fraction of infiltrated Rhine water between the top and bottom sampling depths for all tracers. The values range from 0.71 to 1, with an average of 0.95 and standard deviation of 0.06. Here, the lower values are related to the organic micropollutants, especially the 5-Methyl-Benzotriazole shows smaller fractions. This value however might be affected by the aforementioned 24 hour mixing sample of the infiltrated Rhine water. The highest variability can be observed for the sampling location 21.C.71 where the fraction of infiltrated water

based on isotope data is 100%, organic micropollutants between 14% to 97% and cations and anions between 0% to 96%.

Although uncertainty in terms of the variability in the fraction of infiltrated water has to be assumed for the different tracers, for most locations the calculated ratios are very similar. This can be seen in Figure 7 where the spatial distribution of three tracers is displayed as well as the calculated standard deviation based on all used tracers. The linear interpolation between all sampling points for $\delta^{18}O$, Carbamazepine and HCO_3^- indicates that close to the infiltration channels and ponds (thick white lines) the fraction of infiltrated Rhine water is one. Overall, highest values are obtained for sampling locations in the vicinity of pond 5 and partly of pond 6. In the southern and western part of the study area the fraction of infiltrated water decreases to considerably smaller values. Also in the south-eastern part close to the infiltration channels values smaller than 1 can be observed indicating a higher portion of regional groundwater. Although this is true for all tracers it becomes more obvious when Carbamazepine is considered to calculate the mixing ratios. In terms of uncertainty expressed as the standard deviation, the calculated fraction of Rhine infiltrated water is relatively stable (blue to green colouring) in the middle part of the study area where infiltration rates are highest, directly leading to a high fraction of infiltrated water (see section 4.1). Only in the north-western and south-eastern part the uncertainty is higher. Here, the infiltration rates are relatively small and the water fraction from the regional flow is higher.

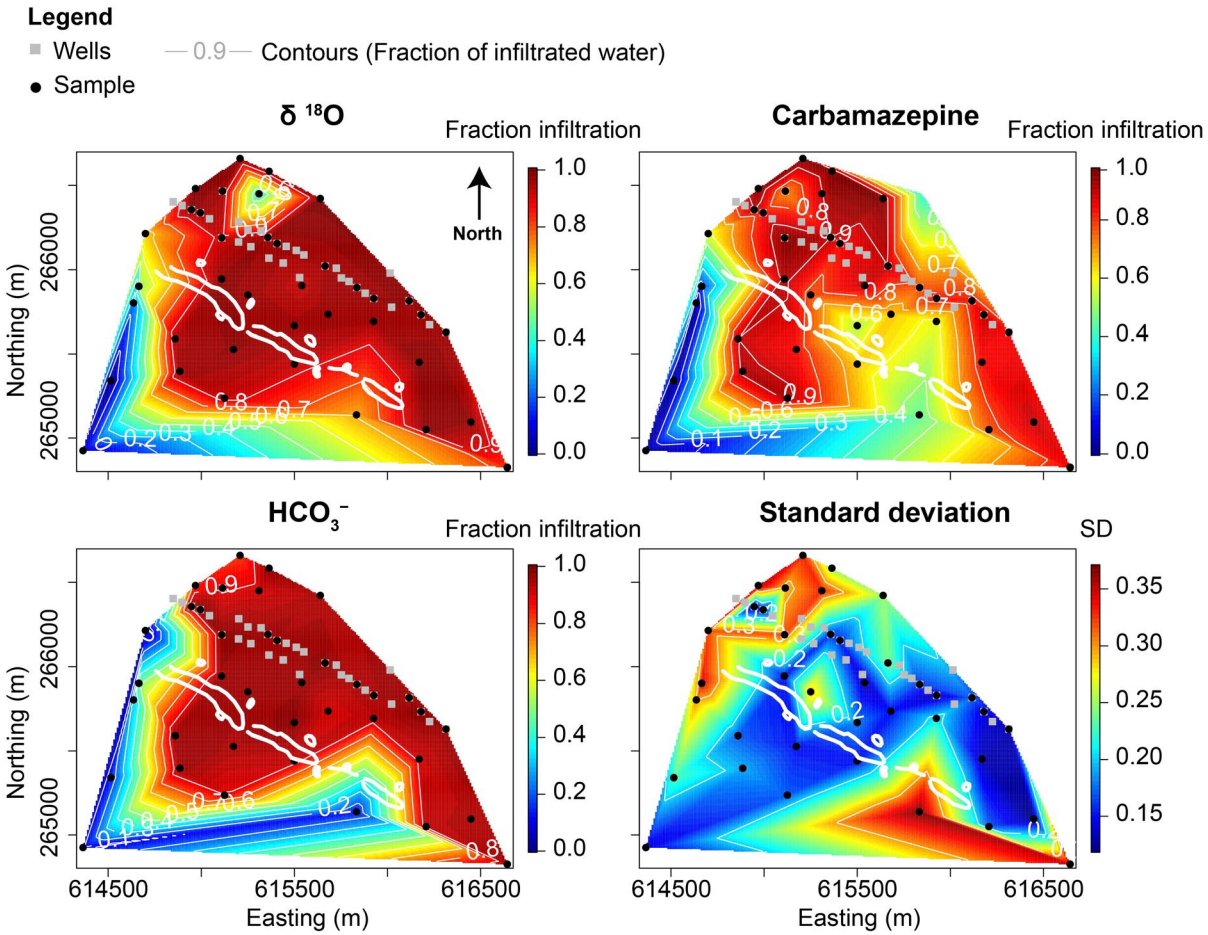

Figure 7: Spatial linear interpolation of mixing ratios (fraction of infiltrated river water) for three selected tracers and for the standard deviation of mixing ratio calculated for all tracers. Red colouring indicates higher fractions of infiltrated Rhine surface water, whereas blue colours present lower fractions. Grey lines show the fraction contours. The solid thick white lines indicate the location of the infiltration channels and ponds.

5. Discussion

In this section we discuss how the selected tracers influence the system understanding. The uncertainties and drawbacks by using different tracers are summarized. Despite uncertainties in the mixing ratio due to measurement and sampling uncertainties the overall spatial distribution of artificial infiltration is very similar for each tracer. That indicates that using only one or a subset of tracers would not change strongly the spatial interpretation of water distribution. Overall, highest infiltration occurred in the eastern part of the infiltration system, located central in the study area. This is in line with results obtained from the stage-discharge relationship and validated the finding from the tracers, confirming that the intended groundwater mound exists between the artificial infiltration system and the pumping well gallery. Small differences in these findings occur however, when Carbamazepine is used.

Using this tracer still the highest infiltration occurred in the eastern part of the infiltration system but with a slightly different spatial pattern compared to most other tracers. For instance, in the south-eastern part close to the infiltration channels values smaller than 1 can be observed indicating a higher portion of regional groundwater. Although this is true for all tracers it becomes more obvious when Carbamazepine is considered to calculate the mixing ratios. In the western part, where the infiltration rates are low and the fraction of infiltrated Rhine water is small, a regional groundwater component is dominating. This result is in line with findings of Moeck et al. [32]. Based on a multivariate statistical analysis the authors found that regional water is also present in drinking water wells in the western part, where water is most likely originating from the south. These wells are therefore of particular interest because here the highest potential risk is given for drinking water supply.

As stated already, the overall spatial distribution is very similar using one or a subset of the tracers but a higher variability of mixing ratios can be observed. Regarding the variability of the mixing ratios two main factors seems to be crucial. First, the sampling strategy and interval can lead to slightly different results. Differences in the concentration of the organic micropollutants are very small (e.g. < 2-16 ng/L, Carbamazepin), where deviations in chemical analyses can lead to pronounced changes in mixing ratio. As we have also seen for the organic micropollutants, a 24 hour mixing sample from the surface water can introduce uncertainty in the calculated mixing ratio. Although Carbamazepine is persistent under conditions during artificial infiltration, uncertainty was introduced due to the variable and unknown input function of the Rhine river water. As demonstrated the load of organic micropollutants in surface water can vary daily and seasonally [40, 41]. This might be of lesser importance when only the spatial distribution is required and differences between surface water and groundwater are large. However, when more precise mixing ratios are needed, times series with small sampling intervals should be chosen compared to single sampling campaigns to ensure the most reliable mixing ratio calculation. This is similar for the stable water isotopes. The Rhine and most other surface waters show at least a seasonal variation in isotope composition. It is therefore fundamental to have good understanding of residence times of artificially infiltrated water. If the residence time is larger than seasonal variability, it might be that the current input signal as an endmember is compared to samples relying on isotope composition from previous seasonal input signals. However, in our case, this might be less important due to the short groundwater residence time of less than 20 days [36] and therefore the stable water isotopes represent the most likely results.

Other factors which might influence our results are precipitation, dissolution and degassing which can occur when the different waters are traveling along the flow path in the subsurface. We observed a wide variability in the mixing ratios when for instance, Ca^{2+}, HCO_3^-, SO_4^{2-} or Na^+ and Cl^- are considered as a tracer for some individual sampling locations. At these locations in the southern and mainly in western part of the study area the fraction of regional groundwater is relatively high. Here, groundwater might have a different mean residence time (age) of up to several years and therefore rock-water interaction might play a more important role then for areas with freshly infiltrated water. Mixing ratios are uncertain at these specific sampling locations based on the cations and anions. Nevertheless, our simple linear calculation helps to identify important areas where further investigations have to be carried out to reduce and constrain uncertainty. For areas where all tracers provide very similar results further sampling is not required. Therefore, multitracer approaches can assist in the design of field data acquisition campaigns, enabling more efficient monitoring strategies, although dissimilar results in absolute mixing ratios are expected.

Furthermore, the obtained results indicate for the study area that a more balanced infiltration between the eastern and western sections of the infiltration system could lead to a better distribution of the elevated local groundwater mound. The western part of the study area which shows under current conditions a larger fraction of regional groundwater might be better protected due to an increase in the fraction of infiltrated water. Moreover, pumping rates at drinking water wells in the western part of the study area where the fraction of regional groundwater is higher should be operated differently and should be investigated in more detail.

6. Summary and conclusions

In this study the distribution of artificially infiltrated Rhine river water into a sand gravel aquifer used for drinking water supply was estimated based on a combined approach of field measurements of infiltration in a channel and pond system and on hydrochemistry data such as main ions, stable water isotopes and organic micropollutants.

Despite uncertainties in the mixing ratio due to measurement and sampling uncertainties the overall spatial distribution of artificial infiltration is very similar for each tracer. Highest infiltration occurred in the eastern part of the infiltration system based on all tracers and infiltration calculation based on stage-discharge relationships. The variability of the mixing ratios between all applied tracers is related to two main factors: The sampling strategy and

interval as well as rock-water interaction. Uncertainty was introduced due to the variable and unknown input function of the Rhine river water because the load of organic micropollutants in surface water can vary daily and seasonally. Furthermore, concentration differences of the organic micropollutants are very small and deviations in the analyses can lead to marked changes in the calculated mixing ratio. Moreover, non-persistent tracers have to be carefully considered to draw conclusions because rock-water interaction can influence the calculated mixing ratio as well. In this study, it was demonstrated that systematically combining a comprehensive data set can help to determine the distribution of artificially infiltrated water and to identify important areas including their uncertainty. At these locations further investigations have to be carried out. The obtained results can assist in the design of field data acquisition campaigns, enabling more efficient monitoring strategies to reduce uncertainty in mixing ratios. Overall, our approach can be easily transferred to a variety of hydrological settings to evaluate the efficiency of managed aquifer recharge for water supply and protection. Using the applied approach leads to more sound conceptual models incorporating also uncertainty, which are acting as the very basis to develop improved water resources management practices in a sustainable way.

Acknowledgments

The authors acknowledge the financial support from the Canton Basel-Landschaft, Switzerland in the framework of the project “Regionale Wasserversorgung Basel-Landschaft 21” as well as internal Eawag Discretionary Funding. This study was further supported by the Competence Centre Environment and Sustainability (CCES) of the ETH domain in the framework of the RECORD Catchment project (Coupled Ecological, Hydrological and Social Dynamics in Restored and Channelized Corridors of a River at the Catchment Scale). We thank Judith Rothardt from Eawag for the measurement of the micropollutants, Caroline Stengel for the measurement of the stable water isotopes and the Eawag AUA lab for measurement of the main cations and anions. We also thank the two anonymous reviewers and the editor for their very valuable comments and suggestions.

References

1. Fletcher TD, Andrieu H, Hamel P. Understanding, management and modelling of urban hydrology and its consequences for receiving waters: A state of the art. Adv Water Resour. 2013;51:261-79.

2. Diamond ML, Hodge E. Urban Contaminant Dynamics: From Source to Effect. Environ Sci Technol. 2007;41:3796-800.

3. Schirmer M, Leschik S, Musolff A. Current research in urban hydrogeology - A review. Adv Water Resour. 2013;51:280-91.
4. Baillieux A, Moeck C, Perrochet P, Hunkeler D. Assessing groundwater quality trends in pumping wells using spatially varying transfer functions. Hydrogeol J. 2015;23:1449-63.
5. Bekesi G, McConchie J. Groundwater recharge modelling using the Monte Carlo technique, Manawatu region, New Zealand. J Hydrol. 1999;224:137-48.
6. Dillon P. Future management of aquifer recharge. Hydrogeol J. 2005;13:313-6.
7. Bouwer H. Artificial recharge of groundwater: hydrogeology and engineering. Hydrogeol J. 2002;10:121-42.
8. Auckenthaler A, Baenninger D, A. A, Zechner E, Huggenberger P. Drinking water production close to contaminant sites: a case study from the region of Basel, Switzerland. GQ10: Groundwater Quality Management in a Rapidly Changing World (Proc 7th International Groundwater Quality Conference held in Zurich, Switzerland, 13–18 June 2010) IAHS Publ 342, 2011, 167-170. 2010.
9. Zoellmann K, Kinzelbach W, Fulda C. Environmental tracer transport (H-3 and SF6) in the saturated and unsaturated zones and its use in nitrate pollution management. J Hydrol. 2001;240:187-205.
10. Bekele E, Patterson B, Toze S, Furness A, Higginson S, Shackleton M. Aquifer residence times for recycled water estimated using chemical tracers and the propagation of temperature signals at a managed aquifer recharge site in Australia. Hydrogeol J. 2014;22:1383-401.
11. Koltermann CE, Gorelick SM. Heterogeneity in sedimentary deposits: A review of structure-imitating, process-imitating, and descriptive approaches. Water Resour Res. 1996;32:2617-58.
12. Moeck C, Hunkeler D, Brunner P. Tutorials as a flexible alternative to GUIs: An example for advanced model calibration using Pilot Points. Environ Modell Softw. 2015;66:78-86.
13. Doherty J. Ground water model calibration using pilot points and regularization. Ground Water. 2003;41:170-7.
14. Abou Zakhem B, Hafez R. Chemical and isotopic methods for management of artificial recharge in Mazraha Station (Damascus Basin, Syria). Hydrol Process. 2012;26:3712-24.
15. Demlie M, Wohnlich S, Ayenew T. Major ion hydrochemistry and environmental isotope signatures as a tool in assessing groundwater occurrence and its dynamics in a fractured volcanic aquifer system located within a heavily urbanized catchment, central Ethiopia. J Hydrol. 2008;353:175-88.
16. Dilsiz C. Conceptual hydrodynamic model of the Pamukkale hydrothermal field, southwestern Turkey, based on hydrochemical and isotopic data. Hydrogeol J. 2006;14:562-72.
17. Xanke J, Goeppert N, Sawarieh A, Liesch T, Kinger J, Ali W, Hotzl H, Hadidi K, Goldscheider N. Impact of managed aquifer recharge on the chemical and isotopic composition of a karst aquifer, Wala reservoir, Jordan. Hydrogeol J. 2015;23:1027-40.
18. Urresti-Estala B, Vadillo-Perez I, Jimenez-Gavilan P, Soler A, Sanchez-Garcia D, Carrasco-Cantos F. Application of stable isotopes (delta S-34-SO4, delta O-18-SO4, delta N-15-NO3, delta O-18-NO3) to determine natural background and contamination sources in the Guadalhorce River Basin (southern Spain). Sci Total Environ. 2015;506:46-57.
19. Widory D, Kloppmann W, Chery L, Bonnin J, Rochdi H, Guinamant JL. Nitrate in groundwater: an isotopic multi-tracer approach. J Contam Hydrol. 2004;72:165-88.
20. Bohlke JK, Smith RL, Miller DN. Ammonium transport and reaction in contaminated groundwater: Application of isotope tracers and isotope fractionation studies. Water Resour Res. 2006;42.

21. Robertson WD, Van Stempvoort DR, Spoelstra J, Brown SJ, Schiff SL. Degradation of sucralose in groundwater and implications for age dating contaminated groundwater. Water Res. 2016;88:653-60.
22. Lee DG, Roehrdanz PR, Feraud M, Ervin J, Anumol T, Jia A, Park M, Tamez C, Morelius EW, Gardea-Torresdey JL, Izbicki J, Means JC, Snyder SA, Holden PA. Wastewater compounds in urban shallow groundwater wells correspond to exfiltration probabilities of nearby sewers. Water Res. 2015;85:467-75.
23. Hillebrand O, Nodler K, Sauter M, Licha T. Multitracer experiment to evaluate the attenuation of selected organic micropollutants in a karst aquifer. Sci Total Environ. 2015;506:338-43.
24. Engelhardt I, Piepenbrink M, Trauth N, Stadler S, Kludt C, Schulz M, Schuth C, Ternes TA. Comparison of tracer methods to quantify hydrodynamic exchange within the hyporheic zone. J Hydrol. 2011;400:255-66.
25. Moschet C, Wittmer I, Simovic J, Junghans M, Piazzoli A, Singer H, Stamm C, Leu C, Hollender J. How a Complete Pesticide Screening Changes the Assessment of Surface Water Quality. Environ Sci Technol. 2014;48:5423-32.
26. Schirmer M, Reinstorf F, Leschik S, Musolff A, Krieg R, Strauch G, Molson JW, Martienssen M, Schirmer K. Mass fluxes of xenobiotics below cities: challenges in urban hydrogeology. Environ Earth Sci. 2011;64:607-17.
27. Van Stempvoort DR, Roy JW, Brown SJ, Bickerton G. Artificial sweeteners as potential tracers in groundwater in urban environments. J Hydrol. 2011;401:126-33.
28. Mawhinney DB, Young RB, Vanderford BJ, Borch T, Snyder SA. Artificial Sweetener Sucralose in U.S. Drinking Water Systems. Environ Sci Technol. 2011;45:8716-22.
29. Huntscha S, Singer HP, McArdell CS, Frank CE, Hollender J. Multiresidue analysis of 88 polar organic micropollutants in ground, surface and wastewater using online mixed-bed multilayer solid-phase extraction coupled to high performance liquid chromatography-tandem mass spectrometry. J Chromatogr A. 2012;1268:74-83.
30. Massmann G, Sultenfuss J, Dunnbier U, Knappe A, Taute T, Pekdeger A. Investigation of groundwater a residence times during bank filtration in Berlin: multi-tracer approach. Hydrol Process. 2008;22:788-801.
31. Gasser G, Pankratov I, Elhanany S, Glazman H, Lev O. Calculation of wastewater effluent leakage to pristine water sources by the weighted average of multiple tracer approach. Water Resour Res. 2014;50:4269-82.
32. Moeck C, Radny D, Borer P, Rothardt J, Auckenthaler A, Berg M, Schirmer M. Multicomponent statistical analysis to identify flow and transport processes in a highly-complex environment. J Hydrol. 2016;542:437-49.
33. Spottke I, Zechner E, Huggenberger P. The southeastern border of the Upper Rhine Graben: a 3D geological model and its importance for tectonics and groundwater flow. Int J Earth Sci. 2005;94:580-93.
34. Affolter A, Zechner E, Huggenberger P. Grundwassermodell Unteres Birstal - Rhein - Muttenz Evaluation der Zuströmbereiche der Trinkwasserfassungen Muttenz und Hardwasser AG Technischer Bericht. 2010; BGA BL-1.
35. Neale PA, Munz NA, Aït-Aïssa S, Altenburger R, Brion F, Busch W, Escher BI, Hilscherová K, Kienle C, Novák J, Seiler T-B, Shao Y, Stamm C, Hollender J. Integrating chemical analysis and bioanalysis to evaluate the contribution of wastewater effluent on the micropollutant burden in small streams. Sci Total Environ. 2017;576:785-95.
36. Otz H. Markierungsversuch 79/80. . Bericht 80-5, Basel-Landschaft, Schweiz. 1980

548 37. Rueedi J, Purtschert R, Beyerle U, Alberich C, Kipfer R. Estimating groundwater mixing ratios
549 and their uncertainties using a statistical multi parameter approach. J Hydrol. 2005;305:1-14.
550 38. Schotterer, U. Wasserisotope in der Schweiz- Neue Ergbnisse und Erfahrungen aus dem
551 nationalen Messnetz ISOT. GWA, 12. 2010
552 39. Scheurer M, Storck FR, Graf C, Brauch HJ, Ruck W, Lev O, Lange FT. Correlation of six
553 anthropogenic markers in wastewater, surface water, bank filtrate, and soil aquifer treatment. J
554 Environ Monitor. 2011;13:966-73.
555 40. Musolff A, Leschik S, Möder M, Strauch G, Reinstorf F, Schirmer M. Temporal and spatial
556 patterns of micropollutants in urban receiving waters. Environ Pollut. 2009;157:3069-77.
557 41. Osenbrück K, Gläser H-R, Knöller K, Weise SM, Möder M, Wennrich R, Schirmer M, Reinstorf
558 F, Busch W, Strauch G. Sources and transport of selected organic micropollutants in urban
559 groundwater underlying the city of Halle (Saale), Germany. Water Res. 2007;41:3259-70.
560